2011 IEEE International Conference on Rehabilitation Robotics
Rehab Week Zurich, ETH Zurich Science City, Switzerland, June 29 - July 1, 2011

Position and Torque Tracking: Series Elastic Actuation versus Model-Based-Controlled Hydraulic Actuation

Alexander Otten,
Wieke van Vuuren,
Arno Stienen,
Edwin van Asseldonk,
Alfred Schouten,
and Herman van der Kooij
Laboratory Biomechanical Engineering
University of Twente
PO Box 217
7500 AE Enschede, The Netherlands
Email: a.otten@utwente.nl

Alfred Schouten
and Herman van der Kooij
BioMechanical Engineering
Delft University of Technology
Delft, The Netherlands

Arno Stienen
Neuro Imaging and Motor Control Laboratory
Northwestern University
Chicago, Illinois

***Abstract*—Robotics used for diagnostic measurements on, e.g. stroke survivors, require actuators that are both stiff and compliant. Stiffness is required for identification purposes, and compliance to compensate for the robots dynamics, so that the subject can move freely while using the robot. A hydraulic actuator can act as a position (stiff) or a torque (compliant) actuator. The drawback of a hydraulic actuator is that it behaves nonlinear.**

This article examines two methods for controlling a nonlinear hydraulic actuator. The first method that is often applied uses an elastic element (i.e. spring) connected in series with the hydraulic actuator so that the torque can be measured as the deflection of the spring. This torque measurement is used for proportional integral control. The second method of control uses the inverse of the model of the actuator as a linearizing controller. Both methods are compared using simulation results.

The controller designed for the series elastic hydraulic actuator is faster to implement, but only shows good performance for the working range for which the controller is designed due to the systems nonlinear behavior. The elastic element is a limiting factor when designing a position controller due to its low torsional stiffness. The model-based controller linearizes the nonlinear system and shows good performance when used for torque and position control. Implementing the model-based controller does require building and validating of the detailed model.

I. Introduction

Stroke is a leading cause of disability commonly resulting in problems coordinating hand and arm movements due to spasticity, synergies, and muscle weakness. Currently, in order to identify the severity and extent of the disability, clinical scales are used that suffer from poor inter rater reliability, are not very sensitive, and cannot identify the underlying pathophysiological mechanisms. Robotics can provide objective diagnostic measures that can be used for identifying underlying pathophysiological mechanisms.

To perform diagnostic measurements, a robotic device should be stiff for identification purposes, yet also compliant to compensate for its own dynamics, so that the subject using the robot can move freely. A diagnostic measurement can be performed while the subject is attached to the robotic device and makes a (predefined) free-reaching movement. During the free movement, a sudden position perturbation is applied during which the subject's response torques are measured. Using identification techniques, properties such as stiffness, damping, inertia, and time delay can be determined that can help explain the underlying pathophysiological mechanisms [1]–[4].

Most robotic devices are currently designed for rehabilitation purposes. The Limpact is a robotic exoskeleton developed at the University of Twente and is designed as a diagnostic measuring device for the upper extremities [5]. The exoskeleton can follow all degrees of freedom of the upper extremity so that subjects can move as naturally as possible. Torques can be applied at the elbow and shoulder joint using rotational hydraulic actuators [6]. Hydraulic, direct-drive actuation is chosen for its high torque-to-weight ratio and fast response.

A hydraulic actuation system behaves nonlinear, and for such a system several control algorithms have been proposed e.g. quantitative feedback control [7], fuzzy logic control [8], active disturbance control [9]–[11], adaptive control [12]–[15] and model-based control [14], [16], [17]. The controller used for diagnostic robotic devices should have a good torque tracking performance for compensating the robot's dynamics or a short rise time when applying a position step function used for diagnostic measurements.

Series elastic actuation (SEA) is often used in diagnostic robots. The hydraulic actuator can therefore be equipped with a spring (i.e. series elastic actuation [6]) where the spring

deflection is measured for the applied torque. Series elastic actuation provides comfortable human machine interaction [18], [19], requires no system knowledge for control and measured torque is equal to applied torque, but the controlled system is still nonlinear limiting performance and stability of the controller to the range for which the controller was designed. Also, the relatively low spring stiffness limits performance of the position controller. As an alternative to SEA control, a model-based (MB) controller can be used. A model-based controller is essentially a torque controller that also linearizes the system so that position control can easily be applied. The MB controller requires detailed system knowledge before it can be implemented. Also, when friction is present and not compensated for, the actuator torque is not equal to the applied torque. Note that for this controller, the connection from actuator to load is rigid i.e. no series elastic element is applied.

The goal is to design a controller for a rotational hydraulic actuator that can provide good torque tracking to compensate for the robot's dynamics, can provide comfortable human machine interaction (e.g. minimal vibrations), and can also provide a basis for a fast-position-controlled system used for diagnostic measurements. A comparison will be made between a conventional proportional integrating (PI) controlled series elastic hydraulic actuator (SEHA) and a MB-controlled hydraulic actuator. The performance of a torque and position controller will be viewed for both systems.

In section II, the physical system will be explained and a mathematical model will be presented. The model-based controller will be designed in section III. Section IV presents the simulated results of model-based controller compared with the results of the PI controller, which uses the torque measurement. The results will be discussed in section V.

II. Modeling of the Setup

A. The hydraulic actuator

The simulations and the MB controller require a detailed model of the test setup of the hydraulic actuator. The setup consists of a hydraulic pump with accumulator that delivers fluid under constant pressure to the control valve. The control valve can regulate the fluid flow to the flexible tubes that connect the valve with the hydraulic actuator. A simplified scheme is depicted in Fig. 1.

The control valve has a built-in controller with a bandwidth of 300 Hz. Due to the relatively high bandwidth, the input signal u can be roughly proportional to the valve position $x_v = K_{ux}u$ with gain K_{ux}.

The fluid flow through the proportional control valve is dependent on the supply pressure P_S, the tank pressure P_T, the pressure at port A P_A and port B P_B and the valve's flow resistance function $K_{v,i}(x_v)$

$$Q_A = K_{v,1}(x_v)\sqrt{P_S - P_A} - K_{v,2}(x_v)\sqrt{P_A - P_T}, \quad (1)$$

$$Q_B = K_{v,3}(x_v)\sqrt{P_B - P_T} - K_{v,4}(x_v)\sqrt{P_S - P_B}. \quad (2)$$

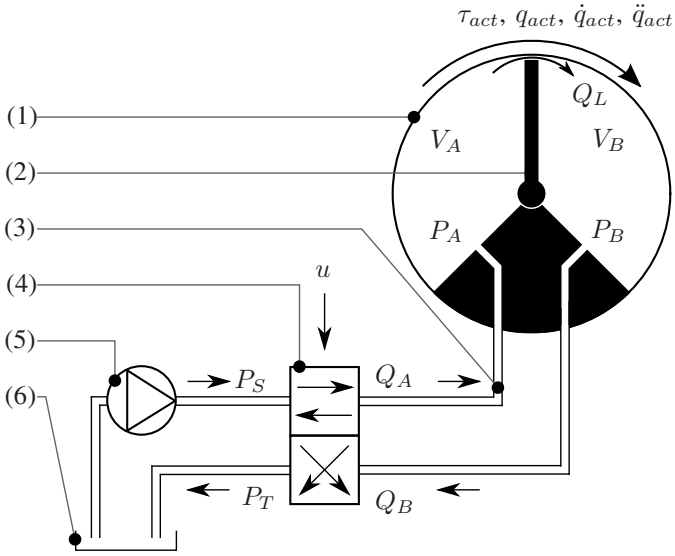

Fig. 1. Scheme of the hydraulic actuator setup which consists of the cylinder (1), the vane (2), the flexible tubes (3), the control valve (4), the pump (5) and the tank (6). The pump delivers oil from the tank at tank pressure P_T to the control valve at the supply pressure P_S. Regulating the control valve with input signal u results in the flows Q_A and Q_B which affects the pressures P_A and P_B in the actuator chambers with volume V_A and V_B. Due to the pressure difference between the two chambers and the small opening between the cylinder wall and the vane, a leakage flow Q_L will occur as well as an actuator torque τ_{act}, displacement q_{act}, velocity $\dot{q}_{act}$ and acceleration $\ddot{q}_{act}$

The valve's flow resistance functions $K_{v,i}(x_v)$ are dependent on the valve position x_v. When the spool clearance is neglected, the valve resistance functions $K_{v,i}(x_v)$ can be written as [17]

$$K_{v,1}(x_v) = \begin{cases} K_c(x_v + d_1), & x_v \geq -d_1, \\ 0, & x_v < -d_1, \end{cases} \quad (3)$$

$$K_{v,2}(x_v) = \begin{cases} K_c(d_2 - x_v), & x_v \leq d_2, \\ 0, & x_v > d_2, \end{cases} \quad (4)$$

$$K_{v,3}(x_v) = \begin{cases} K_c(x_v + d_3), & x_v \geq -d_3, \\ 0, & x_v < -d_3, \end{cases} \quad (5)$$

$$K_{v,4}(x_v) = \begin{cases} K_c(d_4 - x_v), & x_v \leq d_4, \\ 0, & x_v > d_4, \end{cases} \quad (6)$$

with underlap dimensions d_i (opening at $x_v = 0\,\text{m}$) and with constant K_c written as

$$K_c = hC_d\sqrt{\frac{2}{\rho}} \quad (7)$$

with height of the port opening h, discharge coefficient C_d [20] and fluid density ρ.

The time derivatives of the pressure in the chambers are

found to be

$$\dot{P}_A = \frac{\beta_{eff}}{V_r(S+q_{act})+V_{Tube}} \cdot (Q_A - V_r\dot{q} - K_L(P_A - P_B)), \quad (8)$$

$$\dot{P}_B = \frac{\beta_{eff}}{V_r(S-q_{act})+V_{Tube}} \cdot (-Q_B + V_r\dot{q} + K_L(P_A - P_B)), \quad (9)$$

where the total flow consists of the flow due to a valve opening x_v, flow due to a vane velocity $V_r\dot{q}$ with actuator volume per radian V_r and vane velocity $\dot{q}$ and flow due to leaking of seals $K_L(P_A - P_B)$ with leakage resistance K_L and the pressure difference in the actuator $(P_A - P_B)$. The rate of change of (8) and (9) is dependent on the effective bulk modulus β_{eff}, which takes both the fluid and tube stiffness into account, the total volume of the trapped fluid $V_r(S - q_{act}) + V_{Tube}$, which is a function of the angular position of the actuator q_{act} and constants actuator fluid volume per radian V_r, half of the maximum stroke S and fluid volume in the tube V_{Tube}.

The tubes connecting the proportional valve with the actuator are modeled using a lumped approach, see [21] for more information. The fluid dynamics and time delay are incorporated into the model.

B. The mechanical system

The mechanical system consists of two inertias of the actuator and the load that are connected using a torsion spring. The actuation torque is generated by the pressure difference in the actuator and both inertias are subjected to friction torques. A schematic overview is depicted in Fig. 2.

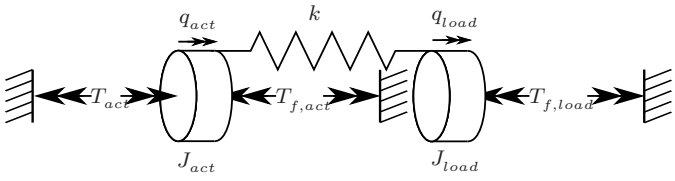

Fig. 2. A schematic overview of the mechanical system where the actuator torque T_{act} is generated by the pressure difference in the actuator, the actuator and the load have inertia J_{act} and J_{load} and an angular rotation of q_{act} and q_{load}, respectively. Both the actuator and the load are subjected to friction torques $T_{f,act}$ and $T_{f,load}$ modeled using a Stribeck friction model [22]–[24]. In the series elastic case, a torsion spring with stiffness k transfers the torques from the actuator to the load. When a model-based controller is used, the connection between the actuator and the load is rigid or $k = \infty$ Nm/rad.

The equation of motion as a function of the angular displacement of the actuator q_{act} and the angular displacement of the load q_{load} can be written as

$$T_{act} - T_{inertia,act} - T_{f,act} - T_{spring} = 0, \quad (10)$$

where

$$T_{act} = V_r(P_A - P_B), \quad (11)$$

$$T_{spring} = J_{act}\ddot{q}_{act}, \quad (12)$$

$$T_{f,act} = \left(T_{c,act} + (T_{s,act} - T_{c,act})e^{-\frac{|\dot{q}_{act}|}{\dot{q}_s}}\right) \cdot \text{sign}(\dot{q}_{act}) + f_v\dot{q}_{act}, \quad (13)$$

$$T_{spring} = k(q_{act} - q_{load}). \quad (14)$$

The friction torque consists of a Coulomb sliding friction torque T_c, a maximum static friction torque T_s, and a viscous friction torque dependent on the angular velocity $\dot{q}$ and the viscous friction factor f_v. The transition from static to viscous friction is dependent on the sliding speed coefficient $\dot{q}_s$. The numerical values are determined experimentally [17].

The equation of motion for the load can also be written down in the same manner as in (10)

$$T_{spring} - T_{inertia,load} - T_{f,load} = 0, \quad (15)$$

with the spring torque T_{spring} as the driving torque. Note that when the model-based controller is implemented, the torsion spring will be replaced by a rigid connection (or $k_{rigid} >> k_{spring}$) resulting in summed inertias, summed friction torques, and no spring deflection or spring torque.

III. Control

The first method of control, which is most often used, consists of a PI controller controlling the series elastic (i.e. torsion) hydraulic actuator (SEHA). The deflection of the torsion spring is used as a measure of torque and is used as control signal for the PI controller. The second method of control is a model-based (MB) controller, which can regulate the pressure difference in the actuator (e.g. torque) and can linearize the system for classical PI position control. Note that the second control method uses a rigid connection between actuator and load.

The controlled actuator should a be able to track a sinusoidal function with an amplitude of 50 Nm of torque up to a frequency of 5 Hz. This is needed for weight support of exoskeleton and arm. For identification purposes, a step function with an amplitude of 50 mrad of angular displacement should have a response with a rise time of 20 ms or less. The delivered torque resolution should be below 1 Nm, and the measured torque resolution below 0.1 Nm.

A. Torque control

For the first method the SEHA has a torsion spring with known stiffness and an encoder measuring the spring deflection. The measured torque can be written as

$$T_{spring} = k(q_{act} - q_{load}) \quad (16)$$

where q_{act} and q_{load} are the rotation of the actuator and the load, respectively and k is the torsion spring stiffness. A block diagram is shown in figure 3. A PI controller is implemented for torque tracking.

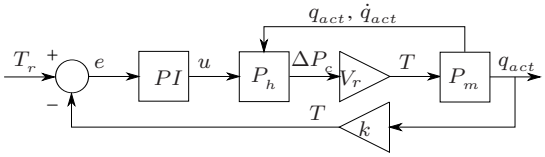

Fig. 3. Torque controller using the spring deflection with P_h and P_m as the hydraulic and mechanical plant, respectively. Note that the load is fixed such that $q_{load} = 0$ rad during torque tracking making the controller effectively a position controller with a gain (i.e. the spring stiffness k) in its feedback loop as shown in figure

For the MB controller, (8) and (9) will be used to determine the time derivative of the pressure difference

$$\Delta\dot{P} = \dot{P}_A - \dot{P}_B = \beta_{eff}\frac{V_{total}}{V_A V_B}(Q_A + Q_B - 2V_r\dot{q} - 2R_L\Delta P), \quad (17)$$

where the total volume V_{total} is the total volume of the actuator (i.e. the volume of the two chambers and both tubes) and the chamber volumes V_A and V_B are the volumes of chamber A and B, respectively.

Combining flow equations (1) and (2) with (17) results in a calculable valve displacement x_v as a function of the pressure difference ΔP

$$x_v(kT+1) = \left[K_{ux}\sum_{i=1}^{4}K_{v,i}(x_v(kT))\right]^{-1} \left[\sum_{i=1}^{4}K_{v,i}(x_v(kT)(-1)^i d_i + \frac{1}{K_c}\left(\frac{V_A V_B}{\beta_{eff}V_{Total}}\Delta\dot{P} + 2V_r\dot{q} + 2R_L\Delta P\right)\right]. \quad (18)$$

with k the current sample and T the sample period. The drawback of (18) is that it contains the time derivative of the pressure difference $\Delta\dot{P}$.

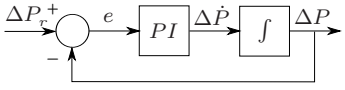

Fig. 4. Block diagram that can be used for estimation of the time derivative of the pressure difference $\Delta\dot{P}$, which is dependent on the reference pressure difference ΔP_r and the measured pressure difference ΔP. The system is tunable using the PI controller.

From Fig. 4, the time derivative of the pressure difference can be replaced by designing the PI controller and setting a preferred pressure difference. The reference pressure difference ΔP_r can now be tracked by tuning the gains of the PI controller, respectively the proportional gain K_p and the integrating gain K_i. This results in a control algorithm that determines the input to the control valve as

$$u(kT+1) = \left[K_{ux}\sum_{i=1}^{4}K_{v,i}(x_v(kT))\right]^{-1} \left[\sum_{i=1}^{4}K_{v,i}(x_v(kT))(-1)^i d_i + \frac{1}{K_c}\left(\frac{V_A V_B}{\beta_{eff}V_{Total}}\left(K_P + K_I\frac{1}{s}\right)(\Delta P_r - \Delta P) + 2V_r\dot{q}_{act} + 2R_L\Delta P)\right] \quad (19)$$

which can be graphically represented as in figure 5

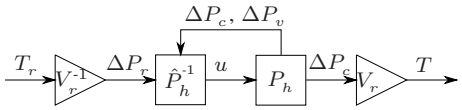

Fig. 5. A block diagram of the model-based, torque-controlled system with P_h as the hydraulic plant and $\hat{P}_h^{-1}$ as the estimate inverse of the plant or model-based controller. Note that the load is fixed and the actuator and load are rigidly connected.

B. Position control

For the first method, a PI position controller is designed for the nonlinear SEHA. The system is described using the equations of motion (10) and (15). A block diagram of the complete controlled system is shown in Fig. 6.

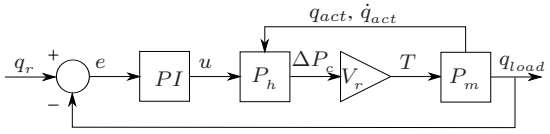

Fig. 6. The nonlinear series elastic hydraulic actuator controlled with a PI controller.

For the second control method, the MB controller is used to linearize the system so that a PI controller can be designed. A block diagram of the complete controlled system is shown in Fig. 7.

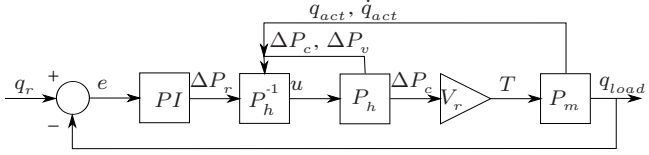

Fig. 7. Linearized system controlled with a PI controller.

IV. Simulation Results

The torque and position controllers are simulated using the nonlinear hydraulic model in Matlab's Simulink. The response to a linear chirp signal (sine wave whose frequency varies linearly with time) is used as a tracking measure for the torque controllers and a step response is used to measure the rise

time of the position-controlled system. Several reference signal amplitudes are used to determine linearity (e.g. consistency of performance). All controllers are designed using the highest input amplitude.

A. Torque Control

The rotational degree of freedom of the load is fixed (i.e. $q_{load} = 0\,\text{rad}$) in order for the spring to be able to deflect and for the pressure to build up. For the pressure difference controller this means that also the rotational degree of freedom of the actuator is fixed (i.e. $q_{act} = 0\,\text{rad}$). The results from the simulations are shown in Fig. 8.

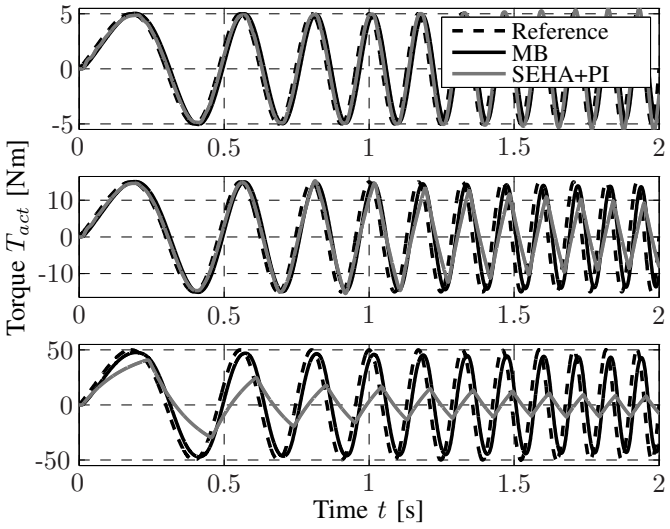

Fig. 8. Torque responses to a linear chirp signal (sine wave whose frequency varies linearly with time). The frequency of the sinusoidal starts at 1 Hz and ends at 10 Hz. Three torque amplitudes of 5, 15 and 50 Nm are used.

The simulation results show that the response of the MB-controlled system is not affected by the different input amplitudes, which is the case for the SEHA PI-controlled system. The latter is due to the systems dynamics, the limited supply pressure, and the nonlinear friction torques. Note that the torque generated by the MB-controlled system is not equal to the applied torque due to actuator friction effects as is the case with the PI-controlled system.

B. Position Control

The first method again uses the PI controller, which is redesigned to control the load angle q_{angle}. The second method uses the MB controller to linearize the system such that a PI controller can be designed for controlling the load angle q_{load}. The simulation results are shown in figure 9.

As can be seen from the simulation results, both systems act nonlinear mostly due to the relative high static friction torques caused by the tight seals, but also due to the fact that at larger rotations, the supply pressure is limiting performance. The SEHA PI-controlled system also shows oscillatory behavior due to the low spring stiffness of the elastic element.

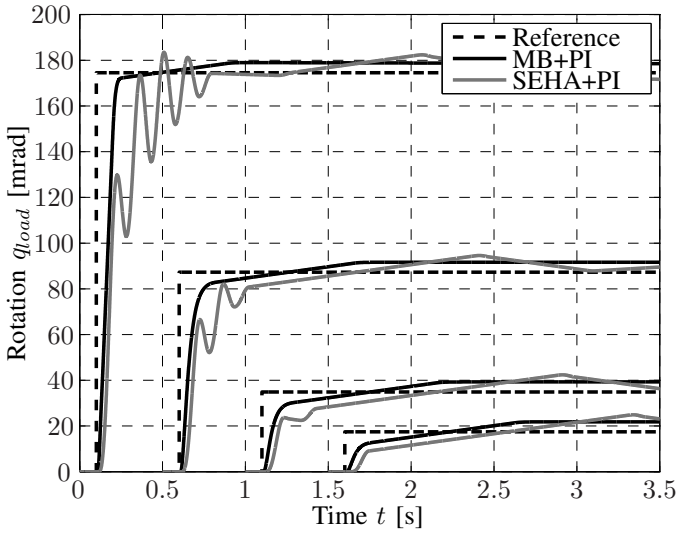

Fig. 9. The step responses PI-controlled SEHA have a rise time (mean $\pm$ standard deviation) of 163 ± 117 ms and an overshoot relative to the input signal of 1.19 ± 0.17. The step responses of the MB-controlled hydraulic actuator have a rise time (mean $\pm$ standard deviation) of 81 ± 13 ms and an overshoot relative to the input signal of 1.11 ± 0.10.

V. Discussion

This article has presented a model of a rotational hydraulic actuator including its proportional valve, tubes, and mechanical dynamic system. The model is first controlled using a conventional proportional integrating (PI) controller in combination with a series elastic hydraulic actuator (SEHA). The elastic element is used for torque measurement. A second model-based (MB) controller is also designed and the performance of both controllers is compared.

The PI-controlled SEHA only has good torque tracking performance at low amplitudes. The performance decreases when higher amplitudes are desired due to friction and hydraulic effects. The MB torque controller shows good torque tracking performance at all amplitudes, which is sufficient for a diagnostic robot. Due to friction effects, the torques generated by the actuator are not equal to the applied torque.

For the position-controlled systems, performance of both controllers is affected by the friction effects causing static errors and a sawtooth-like movement. Both controlled systems also suffer from saturation as the supply pressure is limited. Only the PI-controlled SEHA also shows oscillatory behavior due to the low spring stiffness.

The SEHA PI-controlled system does not seem to meet the requirements according to the simulation results. The MB controller seems promising, especially when higher torques or position steps are demanded. Performance of the MB position controller may be increased by altering the seals in the actuator thus reducing friction and increasing leakage flows or by compensating for friction by using a friction observer [23]. The rise time of the angular step response can be decreased by decreasing the length of the tubes (time delay of 8 ms) and increasing the supply pressure.

Experiments are now being performed for validation of the

model and reduction of friction effects. After that, the MB controller will be implemented.

NOMENCLATURE

C_d	Discharge coefficient	[-]
d_i	Valve underlap dimensions	[m]
f_v	Friction factor	[Nm·s]
h	Height of the valve port opening	[m]
J	Inertia	[kg·m^2]
$K_{v,i}$	Flow functions	[m^3/s/($\sqrt{\text{N/m}^2}$)]
K_{ux}	Relation input voltage to valve position	[m/V]
k	Rotational spring stiffness	[Nm/rad]
Q	Fluid flow	[m^3]
q	Angular position	[rad]
$\dot{q}$	Angular velocity	[rad/s]
P	Pressure	[N/m^2]
R	Resistance	[m^5/Ns]
V_R	Volume per radian	[m^3/rad]
u	Input to proportional control valve	[V]
x	Translational position	[m]
β_{Eff}	Effective bulk modulus	[N/m^2]
ρ	Fluid density	[kg/m^3]

INDICES

A	as an index indicates actuator chamber A
B	as an index indicates actuator chamber B
act	as index indicates actuator
$load$	as an index indicates load
S	as an index indicates supply
T	as an index indicates tank
v	as an index indicates valve
L	as an index indicates leakage
i	as an index indicates underlap opening number
P	as an index indicates proportional control parameter
I	as an index indicates integrating control parameter

ACKNOWLEDGMENTS

The financial support by SenterNovem and provincie Overijsel the Netherlands (grant Pieken in de Delta - Oost Nederland (PIDON), project VirtuRob and grant number 1-5160) is gratefully acknowledged.

REFERENCES

[1] M. A. Krutky, V. J. Ravichandran, R. D. Trumbower, and E. J. Perreault, "Reflex modulation is linked to the orientation of arm mechanics relative to the environment," in *Engineering in Medicine and Biology Society, 2008. EMBS 2008. 30th Annual International Conference of the IEEE*, 2008, pp. 5350 –5353.

[2] M. Krutky, R. Trumbower, and E. Perreault, "Effects of environmental instabilities on endpoint stiffness during the maintenance of human arm posture," in *Engineering in Medicine and Biology Society, 2009. EMBC 2009. Annual International Conference of the IEEE*, 2009, pp. 5938 –5941.

[3] R. D. Trumbower, V. J. Ravichandran, M. A. Krutky, and E. J. Perreault, "Altered multijoint reflex coordination is indicative of motor impairment level following stroke," in *Engineering in Medicine and Biology Society, 2008. EMBS 2008. 30th Annual International Conference of the IEEE*, 2008, pp. 3558 –3561.

[4] R. Kearney, R. Stein, and L. Parameswaran, "Identification of intrinsic and reflex contributions to human ankle stiffness dynamics," *Biomedical Engineering, IEEE Transactions on*, vol. 44, no. 6, pp. 493 –504, 1997.

[5] A. Stienen, "Development of novel devices for upper extremity rehabilitation." Ph.D. dissertation, University of Twente, 2009.

[6] A. Stienen, E. Hekman, H. ter Braak, A. Aalsma, F. van der Helm, and H. van der Kooij, "Design of a rotational hydro-elastic actuator for an active upper-extremity rehabilitation exoskeleton," in *Biomedical Robotics and Biomechatronics, 2008. BioRob 2008. 2nd IEEE RAS EMBS International Conference on*, 2008, pp. 881 –888.

[7] M. Karpenko and N. Sepehri, "Quantitative fault tolerant control design for a leaking hydraulic actuator," *Journal of Dynamic Systems, Measurement, and Control*, vol. 132, no. 5, p. 054505, 2010. [Online]. Available: http://link.aip.org/link/?JDS/132/054505/1

[8] L. Jianxin and T. Ping, "Fuzzy logic control of integrated hydraulic actuator unit using high speed switch valves," in *Computational Intelligence and Natural Computing, 2009. CINC '09. International Conference on*, vol. 1, 2009, pp. 370 –373.

[9] H. Chen, Z. Peng, Y. Fu, and X. Qi, "The application of active disturbance rejection control method to tactical missile electro-hydraulic actuator," in *Electronic Measurement Instruments, 2009. ICEMI '09. 9th International Conference on*, 2009, pp. 3–647 –3–651.

[10] H. Chen, X. Qi, J. Chen, and Y. Fu, "Research on anti-control of missile electro-hydraulic actuator using active disturbance rejection control method," in *Innovative Computing, Information and Control (ICICIC), 2009 Fourth International Conference on*, 2009, pp. 1443 –1446.

[11] C. Yang and Z. Ke, "Study on the active disturbance rejection control of servo system," in *Computer and Communication Technologies in Agriculture Engineering (CCTAE), 2010 International Conference On*, vol. 3, 2010, pp. 364 –367.

[12] E. Wolbrecht, D. Reinkensmeyer, and J. Bobrow, "Pneumatic control of robots for rehabilitation," *The International Journal of Robotics Research*, vol. 29, pp. 23–38, January 2009.

[13] A. Mohanty and B. Yao, "Indirect adaptive robust control of hydraulic manipulators with accurate parameter estimates," *Control Systems Technology, IEEE Transactions on*, vol. PP, no. 99, pp. 1 –9, 2010.

[14] M. Honegger and P. Corke, "Model-based control of hydraulically actuated manipulators," in *Robotics and Automation, 2001. Proceedings 2001 ICRA. IEEE International Conference on*, vol. 3, 2001, pp. 2553–2559.

[15] R. Ghazali, Y. Sam, M. Rahmat, and Zulfatman, "Open-loop and closed-loop recursive identification of an electro-hydraulic actuator system," in *Robotics Automation and Mechatronics (RAM), 2010 IEEE Conference on*, 2010, pp. 285 –290.

[16] P. Chatzakos and E. Papadopoulos, "On model-based control of hydraulic actuators," in *Proc. of RAAD '03, 12th International Workshop on Robotics in Alpe-Adria-Danube Region*, 2003. [Online]. Available: http://citeseerx.ist.psu.edu/viewdoc/summary?doi=10.1.1.75.687

[17] W. v. Vuuren, "Modeling and control of a hydraulic series elastic actuator," Master's thesis, University of Twente, June 2010.

[18] H. Vallery, J. Veneman, E. van Asseldonk, R. Ekkelenkamp, M. Buss, and H. van Der Kooij, "Compliant actuation of rehabilitation robots," *Robotics Automation Magazine, IEEE*, vol. 15, no. 3, pp. 60 –69, 2008.

[19] J. F. Veneman, R. Ekkelenkamp, R. Kruidhof, F. C. van der Helm, and H. van der Kooij, "A Series Elastic- and Bowden-Cable-Based Actuation System for Use as Torque Actuator in Exoskeleton-Type Robots," *The International Journal of Robotics Research*, vol. 25, no. 3, pp. 261–281, 2006. [Online]. Available: http://ijr.sagepub.com/content/25/3/261.abstract

[20] R. von Mises, "Berechnung von ausfluss und berfallzahlen," *Zeitschrift des Vereines Seutscher Ingenieure*, vol. 61, pp. 447–452, 469–473, 493–498, 1917.

[21] T. J. Viersma, *Analysis, synthesis, and design of hydraulic servosystems and pipelines / Taco J. Viersma*.

[22] R. Stribeck, "Die wesentlichen eigenschaften der gleit- und rollenlager the key qualities of sliding and roller bearings," *Zeitschrift des Vereines Seutscher Ingenieure*, vol. 46, pp. 134248, 143237, 1902.

[23] H. Olsson, K. J. Astrom, C. C. de Wit, M. Gafvert, and P. Lischinsky, "Friction models and friction compensation," *Eur. J. Control*, vol. 4, no. 3, pp. 176–195, 1998.

[24] S. Andersson, A. Sderberg, and S. Bjrklund, "Friction models for sliding dry, boundary and mixed lubricated contacts," *Tribology International*, vol. 40, no. 4, pp. 580 – 587, 2007, nORDTRIB 2004. [Online]. Available: http://www.sciencedirect.com/science/article/B6V57-4J2M2Y7-1/2/6e788fbb3a929c752c5977abb105d0c5